Modeled hydraulic redistribution by sunflower (*Helianthus annuus* L.) matches observed data only after including nighttime transpiration

Rebecca B. Neumann[1,2*], Zoe G. Cardon[3], Jennifer Teshera-Levye[1,2], Fulton E. Rockwell[2], Maciej A. Zwieniecki[4,2], N. Michele Holbrook[2]

1. Department of Civil and Environmental Engineering, 201 More Hall, University of Washington, Seattle, WA, 98195
2. Department of Organismic and Evolutionary Biology, 16 Divinity Ave, Harvard University, Cambridge, MA, 02138
3. The Ecosystem Center, Marine Biological Laboratory, 7 MBL Street, Woods Hole, MA, 02543
4. Department of Plant Sciences, 1 Shields Ave, University of California Davis, Davis, CA 95616

*corresponding author: rbneum@u.washington.edu.

Abstract

The movement of water from moist to dry soil layers through the root systems of plants, referred to as hydraulic redistribution (HR), occurs throughout the world and is thought to influence carbon and water budgets and ecosystem functioning. The realized hydrologic, biogeochemical, and ecological consequences of HR depend on the amount of redistributed water, while the ability to assess these impacts requires models that correctly capture HR magnitude and timing. Using several soil types and two eco-types of sunflower (*Helianthus annuus* L.) in split-pot experiments, we examined how well the widely used HR modeling formulation developed by Ryel et al. (2002) matched experimental determination of HR across a range of water potential driving gradients. *H. annuus* carries out extensive nighttime transpiration, and though over the last decade it has become more widely recognized that nighttime transpiration occurs in multiple species and many ecosystems, the original Ryel et al. (2002) formulation does not include the effect of nighttime transpiration on HR. We developed and added a representation of nighttime transpiration into the formulation, and only then was the model able to capture the dynamics and magnitude of HR we observed as soils dried and nighttime stomatal behavior changed, both influencing HR.

Keyword index

hydraulic redistribution, hydraulic lift, *Helianthus annuus*, sunflower, nighttime transpiration, soil texture

Summary Statement

We coupled split-pot hydraulic redistribution (HR) experiments with mathematical modeling to explore the effects of nighttime transpiration on the initiation and maximum

magnitude of HR as soils dry, and the ability of the widely-used Ryel et al. (2002, Oecologia 130: 173-184) model of HR to capture those effects. Using the Ryel formulation, we were unable to match the measured magnitude and pattern of redistribution across a range of water potential driving gradients until we added an empirical representation of nighttime transpiration to the model. The work demonstrates how nighttime transpiration, a process recognized to occur in many species and ecosystems, can diminish the magnitude and alter the pattern of hydraulic redistribution.

Introduction

Hydraulic redistribution, the movement of water from moist to dry soil through the root systems of, primarily, non-transpiring plants, is known to occur in over 60 tree and grass species that grow in xeric, semiarid, temperate and tropical biomes (Caldwell, Dawson & Richards 1998; Horton & Hart 1998; Jackson, Sperry & Dawson 2000; Neumann & Cardon 2012). The process can move water upward, downward and sideways within the soil column, driven by the soil water potential gradient spanning the root system. Both empirical and modeling studies suggest that hydraulic redistribution (HR) can alter carbon and water budgets and ecosystem functioning. The upward movement of water from deep moist soil layers into dry nutrient-rich shallow soil layers where a majority of the root biomass resides can increase dry-season transpiration and photosynthetic rates, maintain or stimulate microbial and/or mycorrhizal activity and increase plant nutrient uptake, maintain soil–root contact, prolong the life span of fine roots, and provide water for seedlings or other shallow-rooted plants. The downward movement of water can facilitate storage of precipitation in deeper soil layers where it does not evaporate (Neumann & Cardon 2012, and references there in).

The manner and extent to which HR impacts hydrologic, biogeochemical and ecological processes depends on the amount of water moved by the root system. For example, a noticeable enhancement of transpiration and photosynthetic rates requires redistribution of a large amount of water (i.e., a significant fraction of the daily transpiration demand and more water moved into dry soil layers than that which can be compensated for by deep roots in moist soil layers) (Domec et al., 2010), while maintenance of soil–root contact and fine root life span requires only a small amount of water (Domec et al. 2004; Bauerle et al. 2008). A recent review of the HR literature (Neumann & Cardon 2012) demonstrates that across 16 different ecosystems, the magnitude of redistribution spans more than two orders of magnitude, from 0.04 to 1.3 mm of water per day in empirical studies and from 0.1 and 3.23 mm of water per day in modeling studies. Notably, modeling studies produce HR estimates that are on the upper end of those derived from empirical studies. The large variation in the magnitude of HR is likely due to variations in site and plant characteristics, as well as to empirical and modeling methodological issues (Neumann & Cardon 2012).

One of the most commonly used models of HR, developed by Ryel et al. (2002), quantifies the magnitude of HR as a function of conductivity along the water flow path and the driving soil water potential gradient between soil layers. The formulation requires few parameters (root biomass distribution, maximum root–soil conductance, the soil water potential where conductance is reduced by 50%, and an empirical constant), and works within the existing framework of large-scale ecosystem models (e.g., Community Land Model (CLM) (Zheng & Wang 2007; Wang 2011), Integrated Biosphere Simulator (IBIS) (Zheng & Wang 2007), Simple Biosphere model (SiB) (Baker et al. 2008), and Australian community land surface model (CABLE) (Li et al. 2012)). Past implementations of the formulation have assumed that during the day, stomata are fully open and thus the soil-to-atmosphere pathway successfully outcompetes the soil-to-soil pathway for available water, and during the night, stomata are fully closed and thus the soil-to-atmosphere pathway does not compete with soil-to-soil pathway for available water (Ryel et al. 2002; Zheng & Wang 2007; Baker et al. 2008; Scholz et al. 2010;

Wang 2011; Li e al. 2012). These assumptions are represented in the formulation with a multiplier (*Dtran*) that is assigned a value of 0 during the day and a value of 1 at night.

Over the last decade, however, it has become widely recognized that nighttime transpiration through stomata occurs in multiple species and many ecosystems (Caird, Richards & Donovan 2007; Dawson et al. 2007), and that nighttime transpiration can reduce redistribution (Howard et al. 2009; Scholz et al. 2008; Domec et al. 2012). The current binary *Dtran* term in the Ryel formulation does not account for this competition between nighttime transpiration (soil-to-atmosphere pathway) and redistribution (soil-to-soil pathway); but competition between the two has important water, carbon and ecosystem implications. For example, water transpired at night rather than redistributed into the soil is not available to enhance next day transpiration and photosynthetic rates, or to stimulate soil biogeochemistry. Further, nighttime transpiration has been shown to reduce water use efficiency since the transpired water is not accompanied by a carbon gain (Caird et al. 2007; Domec et al. 2012). More complex redistribution models developed by Mendel, Hergarten & Neugebauer (2002), Amenu and Kumar (2008), and Siqueira, Katual & Porporato (2008) capture the competition between transpiration and HR, particularly in the context of the diel rhythms of HR and transpiration, but these more complex modeling approaches have not been incorporated into larger-scale models such as CLM, IBIS, SiB, and CABLE. (See Neumann and Cardon (2012) for a review of distinctions among the models).

Using several soil types and two eco-types of *Helianthus annuus* (a species that exhibits nighttime transpiration, Howard & Donovan 2007), we examined how well the original Ryel et al. (2002) formulation matched our experimental determination of HR across a range of water potential driving gradients. The fit of the original model structure was poor, but by developing and adding a representation of nighttime transpiration into the model, it was then able to capture the dynamics and magnitude of HR we observed as soils dried and nighttime stomatal behavior changed.

Material and Methods

We used side-by-side balances to determine the magnitude of water redistributed by wild *Helianthus annus* L. grown in a split-pot configuration (Fig. 1). Below we detail our experimental approach.

Plants, Soils and Growth Conditions

We grew wild *Helianthus annuus* L. from seeds (PI 649859 from California and PI 653547 from New Mexico) obtained from the USDA seed bank (http://www.ars-grin.gov/npgs/), which were sterilized for 15 minutes in 10% bleach solution containing a drop of Tween, and rinsed thoroughly before germination. We sowed seeds in germination trays containing well-watered vermiculite and covered the trays with a plastic lid and tin foil. We placed the trays in a cold room for a period of 15 to 20 days. The tin foil was then removed, and the trays were moved into a growth chamber with 14-hour days (630 to 730 μmoles m^{-2} s^{-1} of light) and 10-hour nights. The temperature and relative humidity remained constant in the growth chamber at 26 ^{o}C and 65%, respectively, resulting in a constant vapor pressure demand (VPD) of 1.17 kPa, day and night. The constant day and night conditions were chosen not to mimic what occurs in the environment but to minimize experimental complications caused by oscillations in temperature and humidity, such as condensation of water vapor on the balance plates. The established vapor pressure demand is representative of the nighttime summer VPD at the locations from which the *H. annuus* seeds were collected.

After seedlings emerged, we gently rinsed their root systems with water to remove attached vermiculite, and transplanted them into specially designed pots constructed out of 3-inch PVC pipe. The pots consisted of two soil-filled sections, each ~ 15 cm tall, connected by a removable section (~2.5 cm long) filled with sandbox sand. We attached a fine mesh cloth to the bottom of the upper soil-filled section and to both the top and bottom of the lower soil-filled section to contain the soil. We used a mesh that was flexible enough for roots to grow through, allowing both the upper and lower soil volumes to become fully populated with roots. Once the plants were fully developed, we gently rinsed out the sand in the removable middle section of the pot, creating two soil-filled pots connected only by roots (Fig. 1).

We used two different types of soil in our experiments: Garden and Arboretum soil. Samples of each were sent to North Carolina State University's (NCSU) Environmental and Agricultural Testing Service Center, where they were analyzed for soil texture (i.e., % sand, % silt, % clay as reported above) and water retention. The Garden soil, obtained from the Harvard University garden, was a sandy soil (91.4% sand, 6.6% silt, 2% clay), with a dark brown/black color and an organic matter content of 7.8% (determined from loss on ignition). The Arboretum soil, obtained from the Harvard University Arboretum, was a sandy loam soil (52.7% sand, 40.5% silt, 6.8% clay) with a light red-brown color and an organic matter content of 7.6% (determined from loss on ignition). We also mixed the Arboretum soil half and half with sandbox sand resulting in a loamy sand (80.1% sand, 15.4% silt, 4.5% clay). Both field soils were sieved through a coarse mesh to remove rocks and other large objects. We packed the soil-filled portions of the pots to achieve a bulk density of approximately 1 g/cm^3 for all soils.

To quantify the relationship between soil water potential and soil water content, we used the SWRC fit web interface (Seki 2007) to fit the NCSU water retention data with Brooks & Corey parameters: $(\frac{\theta-\theta_r}{\theta_s-\theta_r}) = \left(\frac{\Psi}{\Psi_e}\right)^{\lambda}$, where θ is water content, θ_r is residual water content, θ_s is saturated water content, Ψ is soil water potential, Ψ_e is air entry water potential, and λ is a non-dimensional parameter (Brooks & Corey 1964) (Fig. 2). Fitted parameter values are in Table 1.

We used isopiestic psychrometers (Isopiestics Co., Lewes DE) to determine the water potential of the two soils at field capacity. We packed an experimental pot with field soil, thoroughly watered it, and allowed it to drain. Once water was no longer dripping out of the bottom of the pot, we took a sample of the soil and placed it in the psychrometer chamber. We allowed the soil to sequentially equilibrate with a psychrometer holding a drop of 18 MΩ water (0 MPa), a drop of -0.5 MPa sucrose, and no solution (dry) on its junction. The known solutions were used to establish a calibration curve (current versus water potential), and the dry reading was used to determine the sample's soil water potential (Boyer 1995). The relationship between current and water potential is linear, so only two calibration solutions are required (Boyer and Knipling 1965). The Arboretum and Garden soils had a field-capacity water potential of -0.08 MPa and -0.07 MPa, respectively

We conducted hydraulic redistribution experiments using five plants, two grown in Garden soil (PI 653547 from New Mexico), two grown in Arboretum soil (PI 649859 from California), and one grown in the ½ Arboretum: ½ sand mix (PI 649859 from California). For three of these plants, after roots appeared at the bottom of the pot, we laid the pots horizontally in the growth chamber to promote the growth of the plant vertically upwards (Fig. 1a). However, Plant #1 in the Arboretum Soil and the plant in the ½ Arboretum: ½ sand mix were grown vertically, not horizontally. We transitioned to using horizontally grown plants because the resulting leaf and stem configuration for these plants resulted in a smaller spatial footprint for the experimental setup (Fig. 1a and 1b) (see *HR Experiment: Setup*). All plants were watered daily and fertilized with Peters Professional 20-20-20 general-purpose fertilizer (concentration of 250 ppm), as needed. For the horizontal plants, we drilled two access holes into the pots – one in each soil-containing section – to enable watering through 50-ml plastic pipettes.

HR Experiment: Setup

We used the *H. annuus* plants in our hydraulic redistribution experiments after they had grown in the chamber for a period of 1.5 to 3.5 months (see Table 2 for exact ages and other developmentally relevant plant characteristics). In preparations for the HR experiment, the top and bottom of the pots were sealed with multiple layers of Parafilm to limit soil evaporation and water drainage out the ends of the pots. We removed the middle section of the pot and gently rinsed out the sand sandwiched between the two soil-filled pot sections. The two pots, now connected only by roots, were attached with zip-ties to two side-by-side balances (Sartorius model GW6202, 0.01g resolution) using braces Velcroed to the balance plates (Fig. 1a for horizontally grown plants and Fig. 1b for vertically grown plants). To limit evaporation, we wrapped the gap spanned by the roots with plastic that we taped to the two pots. We cut a hole in the bottom of the bag to allow for water drainage, which was caught by a trough laid between the balances. The balances were connected to a computer running Labview (National Instruments) that recorded data from the balances every minute. After attaching the plants to the balances, we checked the weight transfer between pots by systematically placing 200g, 100g and 50g weights on the top and bottom portion of each soil-filled pot section and noting the weight change detected by the adjacent balance. We found the weight transfer between pots ranged from only 0.3% to 1.4% of the applied weight (see SI Table 1).

A few days after placing the plants on the balances, the roots spanning the two pots visually changed. The root surface dried out and turned from a white to brown color, suggesting formation of a suberized layer. Past studies have demonstrated that roots exposed to air develop exodermal suberin lamellae that restrict radial water loss (Clarkson et al. 1987; Enstone & Peterson 1998). The roots remained capable of transporting water, as demonstrated by daily weight changes in the bottom pot (e.g., weight loss during the day).

HR Experiment: Standard Protocol

Our hydraulic redistribution experiments involved drying out the soil in both pots by allowing the plants to transpire for multiple days and nights, watering the top pot to create a water potential difference between the two pots, and monitoring the nighttime weight change in the bottom pot. This approach mimics the process of downward HR in the field, with shallow soil layers receiving water during rain events. We chose to water the top pot because if we had watered the bottom pot, water could have moved through the roots from the bottom pot into the roots of the top pot and then continued up into the aboveground portion of the plant (i.e., leaves and stems). In such a situation, re-hydration of aboveground biomass would have likely dominated any resulting weight change in the top pot. By watering the top pot and watching redistribution in the bottom pot, we minimized the weight contribution of water remaining in the plant biomass (i.e., roots only).

We initiated our experiment by watering both pots to field capacity and zeroing the balances. We withheld water and allowed the plants to transpire until the soil had reached a desired level of dryness. We then bagged both a single leaf and the entire plant top after the lights in the chamber turned off. Five hours after bagging, we cut the bagged leaf and immediately measured its water potential using a pressure chamber (Soil Moisture Equipment Corp., Santa Barbara, CA). We assumed the measured leaf water potential reflected the soil water potential in both pots, since in all of our plants, both pots lost approximately the same amount of water. We then watered the top pot to field capacity, which brought the soil water potential in this pot to -0.07 MPa for the Garden soil and -0.08 MPa for the Arboretum soil — the potentials measured using isopiestic psychrometers for the soils at field capacity. Thus, we created a soil water potential difference between the two pots equal to -0.07 MPa (Garden) or -0.08 MPa (Arboretum) minus the measured leaf water potential. We determined the redistribution rate from the slope of a linear fit to the weight change in the bottom pot over the remainder of the night (see SI Fig. 1 for one example). We left the plant to transpire the following day, and re-watered both pots to field capacity the following night, repeating the experimental sequence after achieving a different level of soil dryness by allowing the plants to transpire for a longer period of time. For our last data point, we cut with scissors and completely removed the roots between the two pots before watering the top pot. We left the plastic bag spanning the gap between the pots in place, and thus, nighttime weight changes measured in the bottom pot for this time point could account for any potential transfer of water vapor across the air gap between the pots (a positive weight change in the bottom pot) and for soil evaporation (a negative weight change in the bottom pot). We found that with the roots cut, the bottom pot lost water (from 0.05 to 0.1 g/hr). We adjusted our calculated HR rates by this measured amount.

Upon completing the experiment, we dissected the pots to determine dry root biomass. We emptied the contents of each pot into a plastic tub, which we filled with water. The soil sank to the bottom of the tub, while the roots floated. We agitated the soil to release the roots, and then captured the floating roots by decanting the water through a fine mesh screen. We refilled the tub multiple times, repeating the process until we had captured a majority of the roots. After removing other floating material from captured roots, we allowed the roots to air dry. Once fully dry, we measured root weight on a balance (Sartorius, 0.0001g resolution).

HR Experiment: Variations to the Standard Protocol

Not all plants experienced exactly the standard protocol, both because the protocol evolved slightly during experiments and because particular pieces of data essential for modeling could not be gathered using the standard protocol. We did not bag the tops of Plant 1 in the Arboretum soil and the plant in the ½ Arboretum: ½ sand mix before collecting leaves for nighttime leaf water potentials (i.e., the leaves used to determine soil water potential of the dry soil). We did, however, bag the leaves used to measure leaf water potential. To account for the difference between leaf water potentials measured with and without bagged tops, we conducted a separate experiment with *H. annuus* plants grown in the same PVC pots packed with the same soils. While drying out the soil in these pots, we first measured leaf water potentials without a bagged top, and then bagged the plant top, and measured leaf water potentials five hours later. We used the resulting linear relationship ($r^2 = 0.91$) between the two leaf water potentials (see SI Fig. 2) to adjust the measured leaf water potentials for these two plants. In addition, we did not cut the roots of these two plants at the end of the HR experiment. Thus, we used the average evaporation rate from the other plants (-0.07 ± 0.03 g/hr) to adjust the calculated HR rates for these two plants.

For Plant 1 in the Arboretum soil, we also did not measure dry root biomass. Instead, after the HR experiment we de-topped this plant to measure well-watered soil–root conductance. We brought the soil up to field capacity, de-topped the plant under water, and sealed it in a Passioura-style root pressure chamber (Passioura and Munns 1984) that we placed on a high-capacity balance (Sartorious, resolution 0.1 g). We measured the flow rate of water out of the plant versus chamber pressure four times over the course of three days. We set the well-watered conductance equal to the slope of the line fitted through the average flow rate (n=4) versus chamber pressure (see SI Fig 3). For the other four plants, we estimated conductance by scaling the measured value for Plant 1 in Arboretum soil by the maximum transpiration rate of each plant (see Table 2). This approach assumes that the maximum transpiration rate of the plants is directly proportional to soil–root conductivity (Becker, Tyree & Tsuda 1999, Lee et al. 2005).

Root-Scale Soil Physics Model

To examine the effect of soil texture alone on the magnitude of HR-associated water flow from a hypothetical single root into our experimental soils, we solved the one-dimensional radial form of Richard's equation $(\frac{\partial\theta}{\partial t}) = \frac{1}{r}\frac{\partial}{\partial r}\left(rK\frac{\partial\Psi}{\partial r}\right)$, where t is time, and r is radial distance from the center of the root (Richards 1931) using a Kircchoff transform ($\Phi = \int_{-\infty}^{\Psi} K d\Psi$, where Φ is the Kircchoff transform variable) (Ross & Bristow 1990) and the pdepe function in MATLAB (http://www.mathworks.com/help/techdoc/). We used our fitted Brooks & Corey parameters for the soil water retention curves (Fig. 2) and default conductivity functions (Rawls, Brakensiek & Saxton 1982) for a sandy loam (Arboretum soil) and sand (Garden soil). All model parameter values are in Table 1. Our boundary conditions included a constant water potential of -0.07 MPa at the soil–root interface, which was set at a radius of 0.05 cm, and constant water potential (equal to the initial water potential) at the outer edge of the soil domain, which was set at a radius of 50 cm to ensure the boundary was sufficiently far from the area of interest. We specified a uniform initial soil water potential for the soil domain, the value of which we varied across simulation runs.

Plant-Scale HR Model

We fit our experimental data to the widely-used Ryel HR formulation (Ryel et al. 2002), which models HR at the whole-plant scale, using the fit function in MATLAB (http://www.mathworks.com/help/techdoc/). The Ryel formulation, as modified by Scholz et al. (2010) is represented as:

$$HR_i = C_{RT} \sum_j \left(\Psi_j - \Psi_i\right) \min\left(c_i, c_j\right) \frac{R_i R_j}{1-R_i} D_{tran} \qquad (1)$$

where HR_i is net water movement into soil layer i from other layers (j), C_{RT} is the maximum radial soil–root conductance of the root system, c_i is a factor ranging from 0 to 1 reducing soil–root conductance based on Ψ_i, R_i is the fraction of active roots in layer i, and D_{tran} is a factor ranging from 0 to 1 reducing redistribution due to transpiration. In previous studies, D_{tran} was operationally set to zero during the day and one during the night (Ryel et al. 2002; Zheng & Wang 2007; Baker et al. 2008; Scholz et al. 2010; Wang 2011; Li e al. 2012). However, Ryel et al. (2002) note that the term could be modified to allow HR to occur when transpiration rates are limited by stomatal conductance. The c_i term is empirically modeled with the relationship:

$$c_i = \frac{1}{1+\left(\frac{\Psi_i}{\Psi_{50}}\right)^b} \qquad (2)$$

where Ψ_{50} is the soil water potential where soil–root conductance is reduced by 50% and b is an empirical constant.

Results

Hydraulic Redistribution Experiments

Figure 3a shows the magnitude of HR as a function of water potential differences between top and bottom pots; data are normalized in Fig. 3b to the measured maximum transpiration rate. In both panels, vertical error bars represent propagated error resulting from adjustments and normalizations made to the data. The error values used in the propagation calculations include two times the standard error of the fitted slope to the nighttime weight data and pot evaporation data (panel A), and two times the standard error of the fitted slope to the nighttime weight data and transpiration data (panel B). Horizontal error bars are estimates of experimental error associated with measuring leaf water potentials (i.e., the difference in pressure at which water was visually seen at stele surface as leaf was pressurized, slightly de-pressurized and then re-pressurized multiple times, and stopping when pressures began to decrease due to water loss from the system). The horizontal error bars for Plant 1 in the Arboretum soil and the ½ Arboretum: ½ sand mix are larger than for the other plants because the tops of these two plants were not bagged before leaves were collected for leaf water potential measurements. Resulting values were adjusted with data comparing leaf water potentials from bagged and unbagged plants (see SI Fig. 2), and the error (standard error on the slope and intercept of the fit) was propagated through this adjustment process. Where noted by symbols in the figure, weight changes for three HR events were not linear (star symbol).

While the magnitude of hydraulic redistribution varied in our experiment, the general pattern of redistribution across water potential driving gradients did not (Fig. 3a). In all five plants, we did not detect HR when water potential differences between the top and bottom pots were small (i.e. when soil in the bottom pot was relatively moist). Instead, even when corrected for evaporation (see Methods), we detected a water loss from the bottom pot, indicating the occurrence of nighttime transpiration. Redistribution, or a weight gain in the bottom pot, did not occur until the soil water potential difference between the two pots increased to 0.7 MPa (i.e., water potential in the bottom pot decreased below -0.7 MPa). In our experiment, after this “initiation” threshold was surpassed, HR increased and reached a peak at a soil water potential difference of 1.5 to 2 MPa. HR then decreased as soil water potential differences continued to increase due to drier soil conditions in the bottom pot.

The maximum amount of HR measured for the five individual plants in our HR experiment ranged from 0.2 to 2 g/hr (Fig. 3a), representing 1 to 14% of the maximum measured whole-plant transpiration rate (Fig. 3b). However, most of the redistributed water was not fully utilized the next day. When the water potential difference between pots was large, the bottom pot continued to gain water during the day though transpiration was active; in the cases when the bottom pot received water during the night and lost water during the day, the amount lost to transpiration was 1.5 to 7 times less than the amount of water redistributed into the pot the previous night. These results suggest that the plant was able to meet its transpiration demand with water from the moist upper pot, and that in our experimental setup, HR did not enhance next day transpiration rates. Further, the results illustrate the competition for water that exists between the soil and atmosphere, with dry soil conditions (i.e., low soil water potentials) in the bottom pot pulling water out of the moist top pot during daytime transpiration. In subsequent sections, we focus on the competition for water between the atmosphere and soil from the perspective of nighttime redistribution. Mainly, the role that nighttime transpiration plays in limiting HR. Both situations highlight that a binary depiction of the impact of transpiration on HR (i.e., setting the D_{tran} term in the Ryel formulation, Eqn. 1, to 0 or 1) does not correctly capture the occurrence of either daytime or nighttime redistribution.

Soil texture and plant characteristics varied in our HR experiments. Our goal was to create combinations of plant and soil that generated a range of magnitudes and patterns in HR, but we were not explicitly testing the effects of soil texture and plant ecotype on HR in, for example, a full factorial design. The California ecotype was grown in the Arboretum and ½ Arboretum: ½ sand mix soils and the New Mexico ecotype was grown in the Garden soil. The impact of soil and plant variation on HR becomes clear when the HR data are normalized by the maximum transpiration rate (Fig. 3b). After the normalization, the points gathered from the two plants in Arboretum soil fall more closely together across the range of water potential differences, and are distinct from points gathered from the two plants in Garden soil and the plant in the ½ Arboretum: ½ sand mix. Based on these normalized data, the New Mexico ecotype in the Garden soil appears to promote proportionally more HR per unit maximum transpiration than the California ecotype in the Arboretum soil, which, in turn, promotes more HR per unit maximum transpiration than the California ecotype in the ½ Arboretum: ½ sand mix.

Root-Scale Soil-Physics Modeling Results

We used a soil physics model to explore how much redistributed water the Arboretum and Garden soils can theoretically accommodate flowing from an individual root as a function of soil water potential. Over a 10-hour period, the model simulated the movement of three orders of magnitude more water into the Arboretum soil than into the Garden soil (Fig. 4a,b). The Garden soil's steeper water retention curve (Fig. 2) limits the movement of water through the soil (i.e., a small change in water content results in a large decrease in soil water potential) while its lower saturated water content and higher residual water content (Table 1) reduces the amount of water the soil can accommodate. However, in the split-pot experiments (Fig. 3a), where soil physics was coupled with variable plant characteristics, the magnitude of water redistributed into the different soil types did not follow that predicted by the soil-physics model. The plants in the Garden soil redistributed more water than the plants in the Arboretum soil.

Plant-Scale HR Modeling Results

The Ryel HR formulation (Ryel et al. 2002), used in many large-scale modeling studies (Ryel et al. 2002; Zheng & Wang 2007; Baker et al. 2008; Scholz et al. 2010; Wang 2011; Li e al. 2012), includes a term that decreases redistribution with soil drying (c_i, which is a function of Ψ_{50} and b, see Eqn. 2). We detected a decrease in HR with soil drying in our experiments (Fig. 3a). However, we were unable to fit our experiment data with the published formulation. Figure 5 shows fits to experimental data given variations in Ψ_{50} and b for Plant 1 in the Arboretum soil, the plant for which we had a measured value of soil–root conductance (i.e., C_{RT}, see Eqn. 1). Regardless of the values of Ψ_{50} and b, the only unknown parameters, the formulation was unable to simultaneously match the magnitude of HR and the water potential difference between pots at which that maximum occurred. For example, Ψ_{50} set at -0.25 MPa approximately captured the appropriate magnitude of maximum HR when b was equal to 1 (Fig. 5a), but when the formulation captured the water potential difference at which the maximum amount of redistribution occurred (x axis ~1.75 MPa, Fig. 5c), it dramatically overestimated the magnitude of maximum HR. The inability of the Ryel formulation to fit our data was not limited to plant 1 in the Arboretum soil. Figure 6 shows the published formulation's best fit to our normalized experimental data sets in the Arboretum and Garden soils (i.e., data normalized by soil–root conductance (C_{RT}, Eqn. 1) see Table 2 for values). The r^2 values for the fits are low (0.35 and 0.23 for the Arboretum and Garden soils, respectively, Table 3).

The poor fit suggests that the Ryel formulation is not accounting for some process or behavior in our experiment that was influencing the magnitude and pattern of redistribution across water potential driving gradients. Our experimental data suggest nighttime transpiration was an important factor. Figure 7 shows that redistribution of water into the bottom pot did not occur when the plants had high rates of nighttime transpiration. Thus, we decided that to correctly represent both the magnitude and pattern of hydraulic redistribution in our experiments, the Ryel et al. (2002) model needed a more complex D_{tran} term that accounted for nighttime transpiration.

We chose to represent nighttime transpiration with an empirical logistical function originally created by Tuzet et al. (2003) to describe the sensitivity of stomata to leaf water potentials during the day. The Tuzet function varies between zero and one, and assumes that stomata remain open when bulk leaf water potentials are near zero and close as leaf water potentials drop. To capture the sensitivity of nighttime stomatal behavior to soil drying observed in the field (e.g. reviewed by Dawson 2007), we slightly modified the function to describe the sensitivity of stomata to the average soil water potential during the night:

$$D_{tran} = 1 - \frac{1+\exp(s_f \psi_f)}{1+\exp(s_f(\psi_f - \psi_s))} \tag{3}$$

where ψ_s is the average soil water potential experienced by the plant (i.e., soil water potential in a soil layer scaled by root biomass fraction), ψ_f is a reference potential, and s_f is a sensitivity parameter. The parameters (ψ_f and s_f) account for the sensitivity of stomata in different species to soil water potential, with larger s_f and ψ_f values signifying greater sensitivity at higher soil water potentials, respectively. The function works well for describing the response of stomata during the night to drying soil conditions, with stomata remaining open enough at moist soil water potentials to allow for nighttime transpiration and closing at drier soil water potentials to limit nighttime transpiration. Simpler D_{tran} formulations, such as a linear response of stomata to soil moisture, did not provide a satisfactory fit to our experimental data. Further, the species-specific flexibility of the Eqn. 3 is important because nighttime stomata conductance can vary substantially among species (Caird et al. 2007). The one minus portion of the right-hand side of Eqn. 3 accounts for the fact that nighttime transpiration limits HR.

After including the modified D_{tran} term to the Ryel formulation, we were better able to fit our experimental data (Fig. 6). The r^2 value for the fit to the Arboretum- and Garden-soil data sets were 0.79 and 0.99, respectively (Table 3). The 95% confidence range for the D_{tran} parameters (i.e., Ψ_f, s_f) from the fit to the Garden-soil data set was narrow, while that from the fit to the Arboretum-soil data set was wide. In fact, the 95% confidence range for the parameters from the Arboretum-soil data set encompassed the parameter values from the Garden-soil data set. Given this overlap and that fact that *Helianthus* species have similar nighttime stomatal conductance (Caird et al., 2007; Howard & Donovan 2007), we chose to further simplify the new model formulation by using the D_{tran} parameters values obtained from the Garden-soil data set to re-fit the Arboretum-soil data set. The result is the dotted line in Fig. 6a — a similar fit to that obtained initially, but with smaller confidence ranges for the fitted parameters (Table 3). Figure 8a shows the fitted D_{tran} and c_i functions for the experimental data sets.

Discussion

Nighttime Transpiration

Data from our redistribution experiments along with our efforts to fit these data with the Ryel HR formulation highlighted the significant influence that nighttime transpiration can have on the magnitude of HR across a range of water potential driving gradients. Past studies focused on the phenomenon of nighttime transpiration have demonstrated both that it can restrict redistribution in *H. annuus* and other species (Howard et al. 2009), and that it is strongly connected to soil moisture and vapor pressure demand (VPD), with more transpiration occurring at moist soil water potentials and high VPD (Dawson et al. 2007; Howard & Donovan 2007). In our experiment, *H. annuus* consistently transpired during the nighttime redistribution events that we stimulated (Fig. 7). The higher nighttime transpiration rates coincided with moist soil conditions in the bottom pot (or with small differences in water potential between the two pots with the top pot always at field capacity during the HR events), aligning with expectations. At these small water potential differences (or moist soil conditions), nighttime transpiration overwhelmed redistribution. Net redistribution did not occur until nighttime transpiration dropped below 1 g/hr (Fig. 7), which coincided with the bottom pot drying out to approximately -0.7 MPa (i.e., a water potential difference of 0.7 MPa, Fig. 3). This type of HR "initiation" threshold has been detected in multiple field studies where HR did not begin until water potentials in the dry soil layer dropped below -0.4 to -0.8 MPa (Ishikawa & Bledsoe 2000; Domec et al. 2004; Meinzer et al. 2004). In our experiment, the threshold appears related to competition for water between soil and nighttime transpiration.

The modified and fitted D_{tran} term (Fig. 8a) accounts for this competition between soil and nighttime transpiration. For small water potential differences (i.e., moist soil conditions in the bottom pot) the fitted D_{tran} term is zero, completely stopping redistribution. As the water potential difference between pots increases (i.e., soil in the bottom pot dries), the term continues to restrict redistribution, though with decreasing impact. The logistical function we used for the D_{tran} term (Eqn. 3) is dependent on soil moisture, and thus, only captures the sensitivity of nighttime transpiration to soil moisture. However, vapor pressure demand also exerts an influence on nighttime transpiration rates (Dawson et al. 2007; Howard et al. 2009; Howard & Donovan 2007). Our experiment did not explicitly test variations of VPD on the rate of HR, as our growth chambers maintained a constant VPD day and night. Inclusion of a VPD response in the D_{tran} term is warranted given the clear impact it can have on nighttime transpiration rates.

Magnitude of HR

The amount of water redistributed by our five experimental plants varied over an order of magnitude, though the same species was grown in identically sized pots under the same climatic conditions. These results highlight the significant impact that natural variations among soils and individual plants can have on the amount of redistributed water— making it difficult to accurately predict and model the amount of redistribution occurring in the environment. A key plant characteristic responsible for some of this variation is soil–root conductance, or the capacity of the plant and soil system to move water. Soil–root conductance estimated from maximum transpiration rates for the five plants varied by a factor of three (Table 1). When the redistribution data were normalized by maximum transpiration, the data sets became more congruent within soil types (Fig. 3b), but an order of magnitude variation still existed in the relative proportion of water redistributed by the plants.

These normalized data highlight the role that soil texture and plant characteristics exert on the magnitude of redistribution. For the same ecotype, an increase in the percent of sand in soil resulted in a decrease in normalized redistribution (Fig. 3b, California ecotype in Arboretum vs. ½ Arboretum: ½ sand soil). This behavior is expected based on published empirical and modeling studies that found sandy soils promote less HR than loamy soils (Schippers, Schroth & Hildebrand 1967; Yoder & Nowak 1999; Siqueira et al. 2008; Wang et al. 2009; Prieto et al. 2010a). However, the New Mexico ecotype, growing in sandier Garden soil, redistributed proportionately more water than the California ecotype growing in loamier Arboretum soil (Fig. 3b), even though our soil physics modeling suggested that the loamier Arboretum soil can accommodate more redistribution than the sandier Garden soil (Fig. 4). These results demonstrate the significant role that plant characteristics play in controlling the magnitude of redistribution. Possible characteristics contributing to the different capacities of the ecotypes to redistribute water include, among others, root biomass (the New Mexico ecotype has more dry root biomass than the California ecotype, Table 2), root diameter and root size distribution, vulnerability of root xylem to embolism, and ability of roots to maintain a connection with to the soil. Only the first characteristic (root biomass) was assessed in our experiment.

Pattern of HR Across Water Potential Driving Gradients

The most striking aspect of our data set was the consistent pattern of redistribution among the five plants, with no redistribution followed by an increase and then decrease in redistribution as the water potential different between pots increased (i.e., the bottom pot dried out) (Fig. 3). Empirical field studies have similarly seen HR increase as soil layers dry, reach a maximum, and then decrease or plateau with continued soil drying (Meinzer et al. 2004; Warren et al. 2005; Scholz et al. 2008; Prieto, Kikvidze & Pugnaire 2010b).

The Ryel et al. (2000) HR formulation, as published, captures the increasing and then decreasing behavior in HR. In the formulation, HR increases as the water potential difference driving flow increases, but as the contributing and/or receiving soil layers dry, the c_i term decreases, reducing the modeled amount of HR (e.g., Fig. 5 and Fig. 8). However, the published formulation does not capture the initial lack of redistribution, nor the magnitude and location of maximum redistribution seen in our experiments. The inclusion of a more complex D_{tran} term that represents the nighttime response of stomata to soil conditions allowed the modeled amount of HR to capture these characteristics. Notably, the inclusion of nighttime transpiration in the formulation reduced the amount of modeled HR and shifted the location of peak HR into drier soil conditions (i.e., larger water potential differences between pots) (Fig. 8b and c).

Acknowledgements

This work was supported by a NOAA Climate and Global Change Postdoctoral Fellowship to RBN, administered by the University Corporation for Atmospheric Research, by a grant from the Andrew W. Mellon Foundation to NMH, and by DOE Terrestrial Ecosystem Science grant ER65389 to ZGC and RBN. We thank Mateusz Zwieniecki for helping with the soil sieving and germination, Janet Sherwood for fertilizing and maintaining the *H. annuus* plants, and Matthew Gilbert for miscellaneous laboratory measurements and many helpful discussions.

References

Amenu G & Kumar P (2008). A model for hydraulic redistribution incorporating coupled soil-root moisture transport. *Hydrology and Earth System Sciences, 12*(1), 55–74.

Baker IT Prihodko L, Denning AS, Goulden M, Miller S & da Rocha HR (2008) Seasonal drought stress in the Amazon: Reconciling models and observations. *Journal of Geophysical Research-Biogeosciences*, 113, G00B01.

Bauerle TL, Richards JH, Smart DR & Eissenstat DM (2008) Importance of internal hydraulic redistribution for prolonging the lifespan of roots in dry soil. *Plant Cell & Environment* 31, 177–186.

Becker P, Tyree MT & Tsuda M (1999) Hydraulic conductances of angiosperms versus conifers: similar transport sufficiency at the whole-plant level. *Tree Physiology* 19, 445–452.

Boyer JS (1995) *Measuring the Water Status of Plants and Soils*. Academic Press, San Diego, 178 pp.

Boyer JS & Knipling EB (1965) Isopiestic technique for measuring leaf water potentials with a thermocouple psychrometer. *Proceedings of the National Academy of Sciences* 54, 1044–1051.

Brooks RH & Corey AT (1964) Hydraulic properties of porous media. *Hydrology Papers.* Colorado State University, Fort Collins, CO.

Caird MA, Richards JH & Donovan LA (2007) Nighttime stomatal conductance and transpiration in C-3 and C-4 plants. *Plant Physiology* 143, 4–10.

Caldwell MM, Dawson TE & Richards JH (1998) Hydraulic lift: Consequences of water efflux from the roots of plants. *Oecologia* 113, 151–161.

Clarkson DT, Bobards AW, Stephens JE & Stark M (1987) Suberin lamellae in the hypodermis of maize (*Zea mays*) roots; development and factors affecting the permeability of hypodermal layers. *Plant Cell & Environment* 10, 83–93.

Dawson TE, Burgess SSO, Tu KP, Oliveira RS, Santiago LS, Fisher JB, Simonin KA & Ambrose AR (2007) Nighttime transpiration in woody plants from contrasting ecosystems. *Tree Physiology* 27, 561–575.

Domec J-C, Warren JM, Meinzer FC, Brooks JR & Coulombe R (2004) Native root xylem embolism and stomatal closure in stands of Douglas-fir and ponderosa pine: mitigation by hydraulic redistribution. *Oecologia* 141, 7–16.

Domec J-C, King JS, Noormets A, Treasure E, Gavazzi MJ, Sun G & McNulty SG (2010) Hydraulic redistribution of soil water by roots affects whole-stand evapotranspiration and net ecosystem carbon exchange. *New Phytologist* 187, 171–183.

Domec, J-C, Ogée J, Noormets A, Jouangy J, Gavazzi M, Treasure E, Sun G, McNulty SG, Kind JS (2012). Interactive effects of nocturnal transpiration and climate change on the root hydraulic redistribution and carbon and water budgets of southern United States pine plantations. *Tree Physiology*, *32*(6), 707–723.

Enstone DE, & Peterson CA (1998) Effects of exposure to humid air on epidermal viability and suberin deposition in maize (Zea mays L.) roots. *Plant Cell & Environment, 21*(8), 837–844.

Horton JL & Hart SC (1998) Hydraulic lift: a potentially important ecosystem process. *Trends In Ecology & Evolution* 13, 232–235.

Howard AR & Donovan LA (2007) Helianthus nighttime conductance and transpiration respond to soil water but not nutrient availability. *Plant Physiology* 143, 145–155.

Howard AR, Van Iersel MW, Richards JH & Donovan LA (2009) Night-time transpiration can decrease hydraulic redistribution. *Plant Cell & Environment*, 32, 1060–1070.

Ishikawa CM & Bledsoe CC (2000) Seasonal and diurnal patterns of soil water potential in the rhizosphere of blue oaks: evidence for hydraulic lift. *Oecologia* 125, 459–465.

Jackson RB, Schenk HJ, Jobbagy EG et al. (2000) Belowground consequences of vegetation change and their treatment in models. *Ecological Applications* 10, 470–483.

Lee JE, Oliveira RS, Dawson TE & Fung I (2005) Root functioning modifies seasonal climate. *Proceedings of the National Academy of Sciences* 102, 17576–17581.

Li L, Wang Y-P, Yu Q, Pak B, Eamus D, Yan J, van Gorsel E & Baker IT (2012) Improving the responses of the Australian community land surface model (CABLE) to seasonal drought. *Journal of Geophysical Research* 117, G04002.

Meinzer FC, Brooks JR, Bucci S, Goldstein G, Scholz FG & Warren JM (2004) Converging patterns of uptake and hydraulic redistribution of soil water in contrasting woody vegetation types. *Tree Physiology* 24, 919–928.

Mendel M, Hergarten S & Neugebauer H. (2002). On a better understanding of hydraulic lift: A numerical study. *Water Resources Research*, *38*(10), 1183, doi:10.1029/2001WR000911.

Neumann RB & Cardon ZG (2012) The magnitude of hydraulic redistribution by plant roots: a review and synthesis of empirical and modeling studies. *New Phytologist* 194, 337–352.

Passioura JB & Munns R (1984) Hydraulic resistance in plants. II. Effects of rooting medium, and time of day, in barley and lupin. *Australian Journal of Plant Physiology* 11, 341-350.

Prieto I, Martínez-Tillería K, Martínez-Manchego L, Montecinos S, Pugnaire FI & Squeo FA (2010a) Hydraulic lift through transpiration suppression in shrubs from two arid ecosystems: patterns and control mechanisms. *Oecologia* 163, 1–11.

Prieto I, Kikvidze Z & Pugnaire FI (2010b) Hydraulic lift: soil processes and transpiration in the

Mediterranean leguminous shrub *Retama sphaerocarpa* (L.) Boiss. *Plant and Soil* 329, 447–456.

Rawls WJ, Brakensiek DL & Saxton KE (1982) Estimation of Soil Water Properties. *Transactions of the ASAE* 25, 1316–1320.

Richards LA (1931) Capillary conduction of liquids through porous mediums. *Physics* 1, 318–333.

Ross PJ & Bristow KL (1990) Simulating water movement in layered and gradational soils using the Kirchhoff transform. *Soil Science Society of America Journal* 54, 1519–1524.

Ryel RJ, Caldwell MM, Yoder CK, Or D., Leffler AJ (2002) Hydraulic redistribution in a stand of *Artemisia tridentata*: evaluation of benefits to transpiration assessed with a simulation model. *Oecologia* 130, 173–184.

Schippers B, Schroth MN & Hildebrand DC (1967) Emanation of water from underground plant parts. *Plant and Soil 27*, 81–91.

Scholz FG, Bucci SJ, Goldstein G. Moriera MZ, Meinzer FC, Domec J-C, Villalobos-Vega R, Franco AC & Miralles-Wilhelm F (2008) Biophysical and life-history determinants of hydraulic lift in Neotropical savanna trees. *Functional Ecology* 22, 773–786.

Scholz FG, Bucci SJ, Hoffmann WA, Meinzer FC & Goldstein G (2010) Hydraulic lift in a Neotropical savanna: Experimental manipulation and model simulations. *Agricultural and Forest Meteorology* 150, 629–639.

Seki K (2007) SWRC fit- a nonlinear fitting program with a water retention curve for soils having unimodal and bimodal pore structure. *Hydrology and Earth System Sciences Discussions* 4, 407–437.

Siqueira M, Katul G & Porporato A (2008) Onset of water stress, hysteresis in plant conductance, and hydraulic lift: Scaling soil water dynamics from millimeters to meters. *Water Resources Research* 44, W01432.

Tuzet A, Perrier A & Leuning R (2003) A coupled model of stomatal conductance, photosynthesis and transpiration. *Plant Cell & Environment*, 26, 1097–1116.

Wang G (2011) Assessing the potential hydrological impacts of hydraulic redistribution in Amazonia using a numerical modeling approach. *Water Resources Research* 47, W02528.

Wang X, Tang C, Guppy CN & Sale PWG (2009) The role of hydraulic lift and subsoil P placement in P uptake of cotton (*Gossypium hirsutum* L.). *Plant and Soil* 325, 263–275.

Warren JM, Meinzer FC, Brooks JR & Domec J-C (2005) Vertical stratification of soil water storage and release dynamics in Pacific Northwest coniferous forests. *Agricultural and Forest Meteorology* 130, 39–58.

Yoder CK & Nowak RS (1999) Hydraulic lift among native plant species in the Mojave Desert. *Plant and Soil* 215, 93–102.

Zheng Z & Wang G (2007) Modeling the dynamic root water uptake and its hydrological impact at the Reserva Jaru site in Amazonia. *Journal of Geophysical Research* 112, G04012.

Table 1. Values for Brooks & Corey Water-Retention Parameters

	θ_s	θ_r	λ	ψ_e (MPa)	K_s (cm/hr)[*]	$\eta=3+2/\lambda$
Arboretum Soil	0.4	0	0.230	-0.0016	30.5	11.7
Garden Soil	0.35	0.06	0.535	-0.0005	32.0	6.7

[*] default values from Rawls et al. (1982) for sandy loam (Arboretum soil) and sand (Garden soil)

Table 2. Characterization of plants used in redistribution experiments

Plant	Maximum Well-Watered Transpiration Rate (g/hr)	Well-Watered Soil–Root Conductance, C_{RT} in Eqn. 1 (g/hr/MPa)	Age of Plant at Start of Exp. (weeks)[a]	Plant Height at Start of Exp. (cm)	Number of leaves at Start of Exp.	Dry Root Biomass at End of Exp. (g)
Arboretum Soil CA Ecotype Plant 1	14.1	12.2	18	n.m.[c]	n.m.	n.m.
Arboretum Soil CA Ecotype Plant 2	6.3	5.5[b]	20	69	~100 small leaves	9.5
Top Pot						5.6
Bottom Pot						3.9
Garden Soil NM Ecotype Plant 1	11.6	10.1[b]	10.5	29	12 big and 28 small leaves	26.3[d]
Top Pot						17.3[d]
Bottom Pot						9.0
Garden Soil NM Ecotype Plant 2	13.6	11.8[b]	10.5	29	12 big and 26 small leaves	25.0[d]
Top Pot						19.6[d]
Bottom Pot						5.4
½ Arboretum: ½ sand CA Ecotype	19.5	16.9[b]	14	45	~125 small leaves	7.8
Top Pot						4.7
Bottom Pot						3.1

[a] Weeks since seeds placed in growth chamber.

[b] Estimated by scaling measured conductance for Plant 1 in Arboretum Soil by the maximum well-watered transpiration rates.

[c] Not measured.

[d] Includes stem below the soil surface.

Table 3. Parameter Values and Statistics for Fit to Ryel HR Formulation

	Soil	**Ψ_{50} MPa**	**95% conf. bounds**	**b**	**95% conf. bounds**	**Ψ_f MPa**	**95% conf. bounds**	**s_f**	**95% conf. bounds**	**sse 10^{-3}**	**r^2**
Night: As published	Arbor. Soil	-0.001	-0.03, 0.03	0.41	-0.79, 1.61					5.8	0.36
	Garden Soil	-0.60	-1.84, 0.64	1.95	-1.58, 5.48					2.7	0.23
Night: Model with nighttime transp.	Arbor. Soil	-1.76	-4.45, 0.92	6.61	-0.91, 14.12	-1.41	-6.17, 3.34	2.92	-16.85, 22.69	2.2	0.76
	Arbor. Soil w/ Garden Param.	-1.56	-1.74, -1.38	6.81	4.43, 9.18	-1.04	n/a	6.68	n/a	2.5	0.73
	Garden Soil	-1.89	-1.92, -1.86	15.28	13.54, 17.03	-1.04	-1.07, -1.00	6.68	5.81, 7.55	.007	0.99

Figure Captions

Figure 1: HR experimental setup for A) horizontally grown plants and B) vertically grown plants.

Figure 2: Water retention curves (i.e., water content versus water potential) for the Garden and Arboretum experimental soils. The closed symbols represent data collected by NCSU Environmental and Agricultural Testing Service Center. The open symbol represents the saturated water content determined from drainage tests. Data were fit with Brooks and Corey parameters. The fit for the Garden soil had an r^2 of 0.99, and the fit for the Arboretum soil had an r^2 of 0.98. Fitted parameter values are in Table 1.

Figure 3: Data from HR experiments. A) Nighttime weight change in the bottom pot versus water potential difference between the two pots. The top pot remained at field capacity for all of the experiments. B) Nighttime weight change in the bottom pot normalized by the maximum, well-watered transpiration rate (see Table 2) versus water potential difference between pots. See text for descriptions of error bars (which, in some cases, are small enough to be hidden underneath symbols).

Figure 4: Results from root-scale soil-physics model. Simulated cumulative nighttime (10-hour) radial flux of water through A) Arboretum and B) Garden soil. X-axis identifies initial water potential for soils. Note the y-axis scale difference for the two panels. C) Soil conductivity functions used in model.

Figure 5: Measured versus modeled HR using Ryel formulation (Eqn. 1) for Plant 1 in the Arboretum soil.

Figure 6: Measured versus modeled HR for experimental data sets normalized by estimated soil–root conductance (Table 2), i.e., C_{RT} term in Ryel formulation (Eqn. 1) A) Plants in arboretum soil. B) Plants in Garden soil. Grey line indicates best fit to data using unmodified Ryel formulation. Black lines indicate best fit to data with nighttime transpiration modification (Eqn. 3). Dotted black line indicates fit to data from plants in Arboretum-soil data using parameters developed from plants in Garden soil.

Figure 7: Relationship between nighttime weight change in bottom pot and nighttime transpiration for all five experimental plants.

Figure 8: Summary of experimental and modeling results. A) Fitted functions for c_i and D_{tran} terms in the Ryel formulation (Eqns. 1, 2, and 3) based on experimental data. B & C) Modeled redistribution normalized by soil–root conductance (i.e., C_{RT} in Eqn. 1) for plants in B) Garden and C) Arboretum soil both with and without nighttime transpiration (i.e., inclusion of D_{tran}).

Figure 1

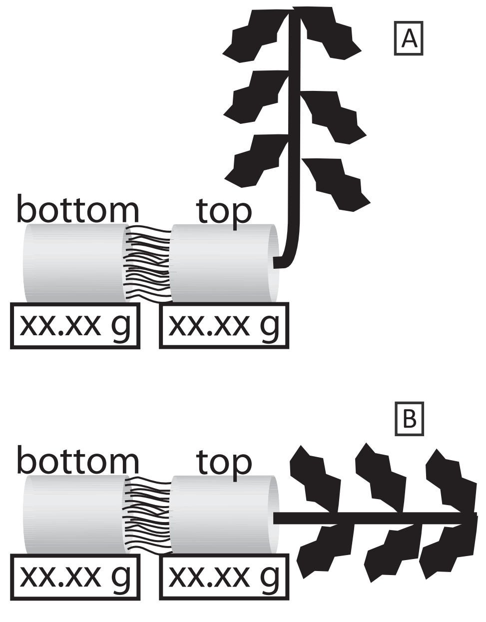

Figure 2

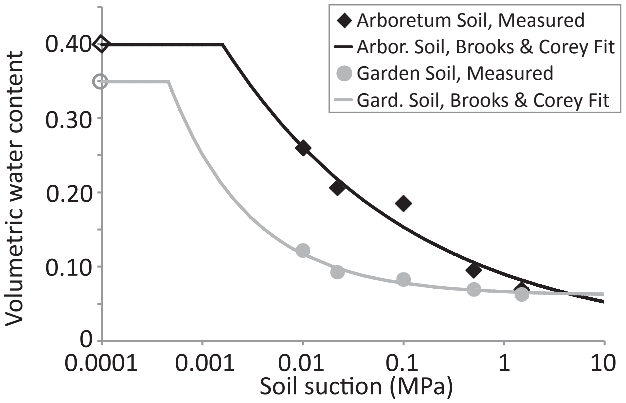

◆ Arboretum Soil, Measured
— Arbor. Soil, Brooks & Corey Fit
● Garden Soil, Measured
— Gard. Soil, Brooks & Corey Fit
Volumetric water content
0.40
0.30
0.20
0.10
0
0.0001
0.001
0.01
0.1
1
10
Soil suction (MPa)

Figure 3

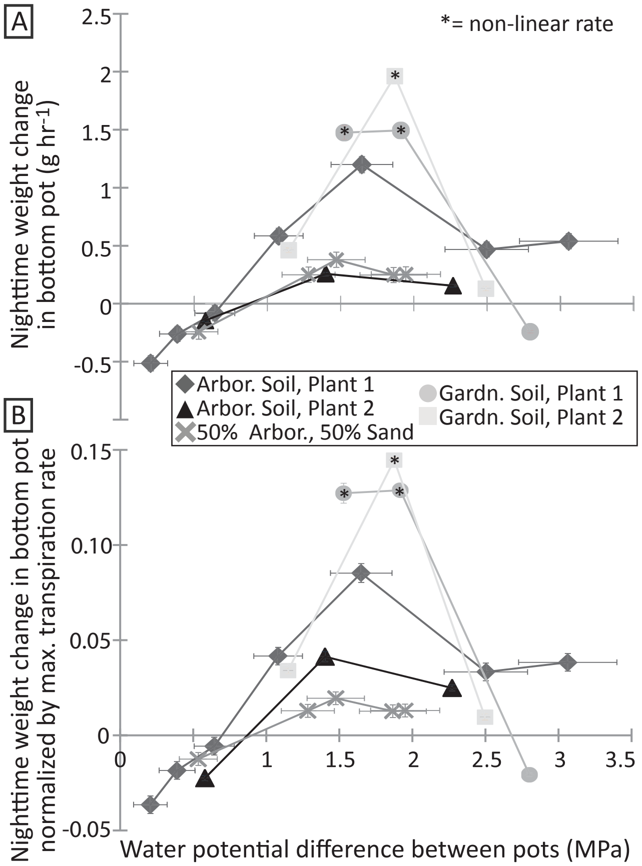
A
*= non-linear rate
Nighttime weight change in bottom pot (g hr-1)
2.5
2
1.5
1
0.5
0
-0.5
Arbor. Soil, Plant 1
Arbor. Soil, Plant 2
50% Arbor., 50% Sand
Gardn. Soil, Plant 1
Gardn. Soil, Plant 2
B
Nighttime weight change in bottom pot normalized by max. transpiration rate
0.15
0.10
0.05
0
-0.05
0
1
1.5
2
2.5
3
3.5
Water potential difference between pots (MPa)

Figure 4

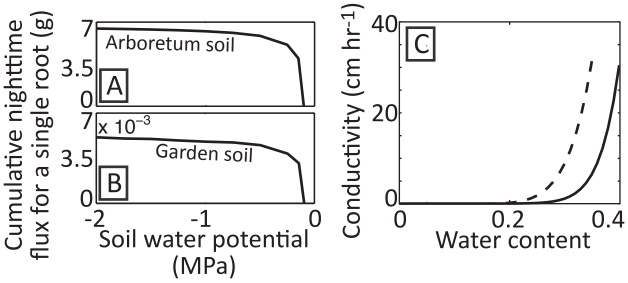

Cumulative nighttime flux for a single root (g)
7
3.5
0
Arboretum soil
A
7
x 10^−3
3.5
0
Garden soil
B
-2
-1
0
Soil water potential (MPa)
Conductivity (cm hr-1)
40
20
0
C
0
0.2
0.4
Water content

Figure 5

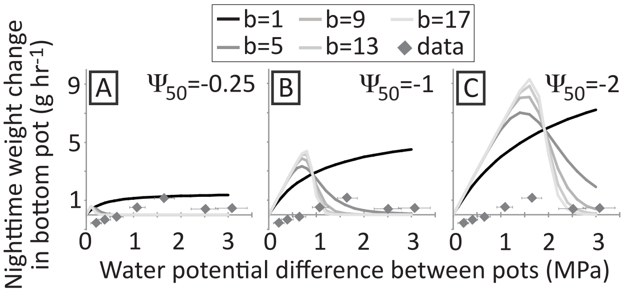
b=1
b=9
b=17
b=5
b=13
◆ data
Nighttime weight change in bottom pot (g hr-1)
A
Ψ_{50}=-0.25
B
Ψ_{50}=-1
C
Ψ_{50}=-2
9
5
1
0
1
2
3
0
1
2
3
0
1
2
3
Water potential difference between pots (MPa)

Figure 6

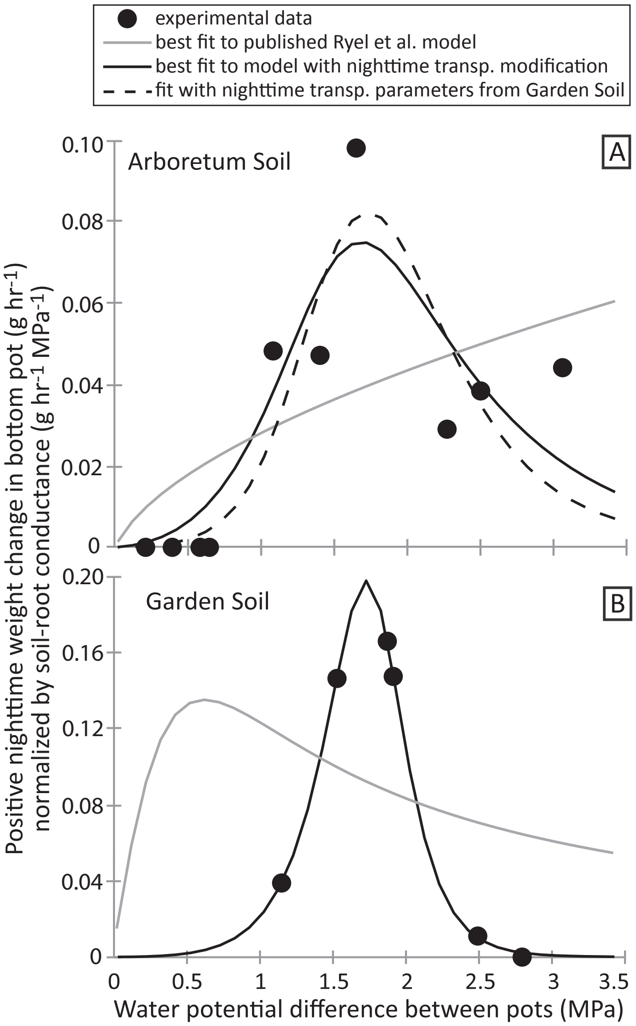

● experimental data
best fit to published Ryel et al. model
best fit to model with nighttime transp. modification
fit with nighttime transp. parameters from Garden Soil
Arboretum Soil
A
0.10
0.08
0.06
0.04
0.02
0
Garden Soil
B
0.20
0.16
0.12
0.08
0.04
0
0
0.5
1
1.5
2
2.5
3
3.5
Positive nighttime weight change in bottom pot (g hr-1) normalized by soil-root conductance (g hr-1 MPa-1)
Water potential difference between pots (MPa)

Figure 7

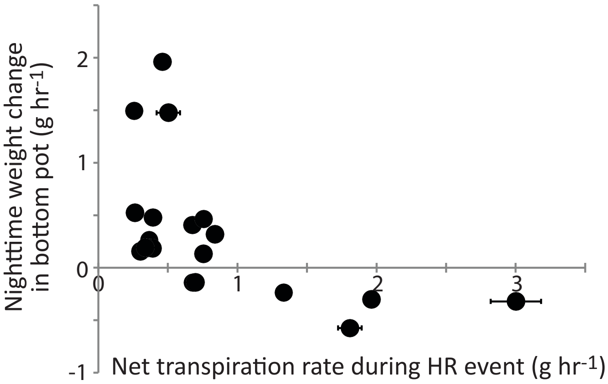
Nighttime weight change in bottom pot (g hr^{-1})
2
1
0
-1
0
1
2
3
Net transpiration rate during HR event (g hr^{-1})

Figure 8

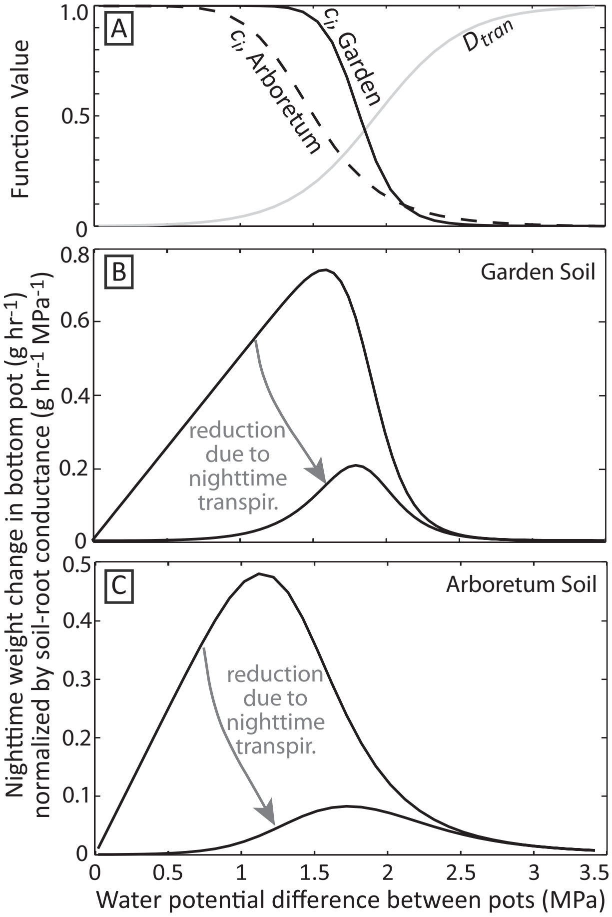

A
1.0
0.5
0
Function Value
c_i, Garden
c_i, Arboretum
D_{tran}
B
Garden Soil
0.8
0.6
0.4
0.2
0
reduction due to nighttime transpir.
C
Arboretum Soil
0.5
0.4
0.3
0.2
0.1
0
reduction due to nighttime transpir.
Nighttime weight change in bottom pot (g hr^{-1}) normalized by soil-root conductance (g hr^{-1} MPa^{-1})
0
0.5
1
1.5
2
2.5
3
3.5
Water potential difference between pots (MPa)